Sharp cutoff versus smooth filtering in large eddy simulation

Giuliano De Stefano[a)]
Dipartimento di Ingegneria Aerospaziale, Seconda Universitá di Napoli, 81031 Aversa, Italy

Oleg V. Vasilyev[b)]
Department of Mechanical and Aerospace Engineering, University of Missouri–Columbia, Columbia, Missouri 65211

(Received 11 January 2001; accepted 3 October 2001)

The large eddy simulation (LES) equations of turbulent flows are formally derived by applying a low-pass filter to the Navier–Stokes equations. As a result the subgrid-scale (SGS) stress tensor strongly depends on the assumed filter shape, which causes a SGS model to be filter dependent. In particular, depending on the choice of the filter the corresponding SGS model should satisfy very different requirements in terms of large scale dynamics and kinetic energy budget. This paper is an attempt to systematically study the effect of the filter shape on the subgrid scale model and its subsequent effect on LES. For the sake of simplicity, we consider numerical simulation of a one-dimensional homogeneous flow, governed by the viscous Burgers equation. Large eddy simulations of the solution of the Burgers problem are performed using subgrid scale models obtained by filtering data from direct numerical simulations. Diagnostics include temporal evolution of energy and dissipation as well as energy spectra. It is demonstrated both theoretically and numerically that the assumed filter shape can have a significant effect on LES in terms of spectral content and physical interpretation of the solution. The results are generalized for LES of three-dimensional turbulent flows and specific recommendations for the use of filters and corresponding SGS models are made.
[DOI: 10.1063/1.1421368]

I. INTRODUCTION

The large eddy simulation (LES) equations of turbulent flows are formally derived by applying a low-pass filter to the Navier–Stokes equations and assuming that filtering and differentiation operators commute. The resulting equations have the same structure as the original equations plus additional terms, called subgrid scale (SGS) stresses. The filtered equations are used to compute the dynamics of the large scale structures, while the effect of the small scale turbulence is modeled using a SGS model. The motivation behind LES is the recognition that the large scales of the turbulence often dominate mixing, heat transfer, and other quantities of engineering interest, while the small scales are only of interest because of how they affect the large ones. Furthermore, large scales are not universal and vary from problem to problem, while small scales exhibit a more or less universal behavior, which considerably simplifies the task of finding the model for the SGS stresses.

The filter width as well as the details of the filter shape are free parameters in LES and these can be used both to control the effective resolution of the simulation and to establish the relative importance of different portions of the resolved spectrum. However, due to the lack of a straightforward and robust filtering procedure for inhomogeneous flows, most large eddy simulations performed to date have not made use of explicit filtering. The nearly universal approach for LES in complex geometries is to argue that the finite support of the computational mesh together with the low-pass characteristics of the discrete differencing operators effectively act as a filter. This procedure is typically referred to as implicit filtering since an explicit filtering operation never appears in the solution procedure. Although the technique of implicit filtering has been used extensively in the past, there are several compelling reasons to adopt a more systematic approach. Foremost of these is the issue of consistency. While it is true that discrete derivative operators have a low-pass filtering effect, the associated filter acts only in the *one spatial direction* in which the derivative is taken. This fact implies that each term in the Navier–Stokes equations is acted on by a distinct one-dimensional filter, and thus there is no way to derive the discrete equations through the application of a single three-dimensional filter. Considering this ambiguity in the definition of the filter, it is nearly impossible to make detailed comparisons of LES results with filtered experimental data.

The second significant limitation of the implicit filtering approach is the inability to control numerical error. Without an explicit filter, there is no direct control in the energy in the high frequency portion of the spectrum. Significant energy in this portion of the spectrum coupled with the nonlinearities in the Navier–Stokes equations can produce significant aliasing error. Furthermore, all discrete derivative operators become rather inaccurate for high frequency solution components and this error interferes with the dynamics of the small scale eddies. This error can be particularly harmful[1] when the

[a)]Electronic mail: giuliano.destefano@unima2.it
[b)]Electronic mail: VasilyevO@missouri.edu

dynamic model[2,3] is used since it relies entirely on information contained in the smallest resolved scales.

The difficulties associated with the implicit filtering approach can be alleviated by performing an explicit filtering operation as an integral part of the solution process.[4,5] By damping the energy in the high frequency portion of the spectrum it is possible to reduce or eliminate the various sources of numerical error that dominate this frequency range. Explicit filtering reduces the effective resolution of the simulation, but allows the filter shape and size to be chosen independently of the computational mesh. Having the ability to control the filter shape opens the whole new horizons in LES modeling, since it makes it feasible to look at SGS modeling and filtering as one inseparable issue.

The success of the large eddy simulations depends on the ability of the SGS model to accurately represent the effect of the unresolved scales on the resolved ones. However, both the definition of resolved scales and the model for the SGS stress tensor, $\tau_{ij}=\overline{u_i u_j}-\overline{u}_i\overline{u}_j$, strongly depend on the assumed filter shape. If the low-pass filter is exactly the sharp cutoff or close to it, then there is a clear separation of scales into large (resolved) and small (unresolved) ones and SGS stresses represent the effect of small (filtered out) scales on large ones. However, if the filter is smooth like Gaussian or top-hat filter, then the boundary between resolved and unresolved scales is not well defined and the resulting SGS stresses represent the effect of small- as well as large-scale interactions. The fact that a portion of large-scale interaction needs to be modeled considerably complicates the modeling effort. One way to deal with this difficulty is to use Bardina's scale similarity models[6] or the tensor-diffusivity models.[7–10] These models exhibit very high levels of correlation (up to 0.97) with exact SGS stresses computed from both the direct numerical simulations (DNS) and experimental data (e.g., Refs. 11–15). The results of an *a priori* test are not that surprising, since these models can be viewed as a way for the *reconstruction* of the filtered large scales interaction, i.e., the Leonard term,[9] $\overline{\overline{u}_i\overline{u}_j}-\overline{\overline{u}}_i\overline{\overline{u}}_j$. However, these models do not provide proper dissipation to be used alone as SGS models (e.g., Refs. 16 and 17). To cure this defect, a number of mixed models have been proposed,[14,16–23] where scale-similarity or tensor-diffusivity models are complemented by Smagorinsky[24] or hyperviscosity[25] models. Both Smagorinsky and hyperviscosity models exhibit low level correlation in *a priori* tests (e.g., Refs. 12–15), yet they provide sufficient dissipation. It was demonstrated in a number of tests[14–18,26] that mixed models work quite well when smooth filter is used. However, when a sharp cutoff (or close to it) filter is used, mixed models reduce to essentially Smagorinsky or hyperviscosity models.

The present paper is mainly intended to demonstrate the importance of looking at filtering and SGS modeling as one inseparable issue and to provide LES practitioners a reference for interpreting the results of their simulations. Moreover, the knowledge of how the filter shape affects LES results is of great importance in constructing efficient and consistent turbulence models. Thus, the objective of the present study is to establish the general framework for looking at the effect of the filter shape on the large scale dynamics and energy transfer. For simplicity reasons we consider one-dimensional homogeneous flow governed by the viscous Burgers equation. The latter equation was originally proposed as a model equation for turbulence in Ref. 27 and can be usefully adopted for SGS modeling studies (e.g., Ref. 28).

The rest of the paper is organized as follows. Section II is devoted to the analysis of large scale dynamics from a theoretical point of view, paying particular attention to the kinetic energy budget. In Sec. III some numerical experiments are presented and results from both DNS and LES are discussed. Finally, in Sec. IV some conclusions are drawn.

II. LARGE SCALE DYNAMICS

In this section the effect of the filter shape is studied from a theoretical point of view. For simplicity reasons we consider one-dimensional homogeneous flow governed by the viscous Burgers equation. Despite the simplicity of the equation, the analysis and subsequent conclusions drawn from it are applicable for the general LES.

Let us consider a one-dimensional homogeneous flow governed by the viscous Burgers equation for the unknown velocity variable $u(x,t)$:

$$\frac{\partial u}{\partial t}+u\frac{\partial u}{\partial x}=\nu\frac{\partial^2 u}{\partial x^2}, \tag{1}$$

where ν stands for the viscosity coefficient. As usual, defining the filtering operation as a spatial convolution, the LES field is given by

$$\overline{u}(x,t)=\int_{x'+x''=x} G(x')u(x'',t)dx', \tag{2}$$

where G is a filter function with a uniform width. Application of filter (2) to Eq. (1) results in the following LES equation describing the evolution of the filtered field:

$$\frac{\partial \overline{u}}{\partial t}+\overline{u}\frac{\partial \overline{u}}{\partial x}=\nu\frac{\partial^2 \overline{u}}{\partial x^2}-\frac{1}{2}\frac{\partial \tau}{\partial x}, \tag{3}$$

where

$$\tau(x,t)=\overline{u^2}-\overline{u}^2 \tag{4}$$

stands for the SGS stress. Thus, the effect of the unresolved scales appears through a source term in the dynamics equation. This term must be modeled in order to close the problem for the unknown filtered velocity $\overline{u}(x,t)$.

In wave number space the filtering operation (2) becomes $\widehat{\overline{u}}(\kappa,t)=\hat{G}(\kappa)\hat{u}(\kappa,t)$, where $\hat{G}$ denotes the Fourier transform of the filter. From a physical point of view, one would like to follow the dynamics of flow structures down to a given size, i.e., to solve the velocity field up to a certain characteristic wave number. Thus, the most natural choice for the filter function is the sharp cutoff filter in Fourier space. This way, the velocity fluctuation $(1-\hat{G})\hat{u}$ does not contain resolved wave number components and the resolved velocity field has a clear physical meaning. On the other hand, smooth filters provide an overlapping between resolved and unresolved scales and the physical interpretation of the large-eddy field is much less clear.

In order to analyze the effect of the filter shape consider the SGS stress spectrum. At a given time instant, the latter is given by

$$\hat{\tau}(\kappa)=\int_{\kappa'+\kappa''=\kappa}[\hat{G}(\kappa)-\hat{G}(\kappa')\hat{G}(\kappa'')]\hat{u}(\kappa')\hat{u}(\kappa'')d\kappa'. \tag{5}$$

Equation (5) is valid for both smooth and sharp cutoff filters. When a sharp cutoff at κ_c is considered, the corresponding SGS stress spectrum can be rewritten as

$$\hat{\tau}(\kappa)=\int_{\kappa'+\kappa''=\kappa}\hat{u}(\kappa')\hat{u}(\kappa'')d\kappa' - \int_{\substack{\kappa'+\kappa''=\kappa \\ |\kappa'|,|\kappa''|\leqslant\kappa_c}}\hat{u}(\kappa')\hat{u}(\kappa'')d\kappa'. \tag{6}$$

For $|\kappa|\leqslant\kappa_c$, the spectrum of $\hat{\tau}$ exactly accounts for the effect of small scales on large ones.

When a smooth filter is adopted, one can define a characteristic wave number, say $\overline{\kappa}$, in order to refer to scales at $|\kappa|\leqslant\overline{\kappa}$ as large ones. For example, for top-hat filtering, one can consider $\overline{\kappa}=\pi/\Delta$, Δ being the characteristic filter width. In this case, the filtered velocity can be defined as $\overline{u}(x,t)=(1/\Delta)\int_{x-\Delta/2}^{x+\Delta/2}u(\xi,t)d\xi$ and the corresponding transfer function is $\hat{G}(\kappa)=\sin(\kappa\Delta/2)/(\kappa\Delta/2)$. For smooth filters the SGS stress accounts not only for the effect of small scales, but also for the effect of filtering on large ones. In fact, if we assume that $\overline{\kappa}=\kappa_c$ and the velocity spectrum does not involve wave numbers beyond this threshold, then, as expected, the SGS stress for the spectral cutoff (6) vanishes while, on the contrary, for a smooth filter, Eq. (5) provides a nonzero SGS stress, since $\hat{G}(\kappa'+\kappa'')\neq\hat{G}(\kappa')\hat{G}(\kappa'')$.

The matter is better understood by considering the kinetic energy decay. Consider the energy budget in wave number space

$$\frac{\partial E}{\partial t}=-2\nu\kappa^2E+T, \tag{7}$$

where $E(\kappa,t)=|\hat{u}|^2$ is the energy density spectrum and $T(\kappa,t)=-\kappa\Im[\hat{u}^*(\hat{u}\star\hat{u})]$ represents the energy transfer among different wave numbers. Note that $(\cdot)^*$ denotes complex conjugation, while $\hat{u}\star\hat{u}\equiv\int_{\kappa'+\kappa''=\kappa}\hat{u}(\kappa',t)\hat{u}(\kappa'',t)d\kappa'$ stands for the convolution in Fourier space.

When the filtered field is considered, one obtains

$$\frac{\partial\mathcal{E}}{\partial t}=-2\nu\kappa^2\mathcal{E}+\mathcal{T}+\mathcal{P}, \tag{8}$$

where $\mathcal{E}(\kappa,t)=|\hat{\overline{u}}|^2$ is the resolved field energy, $\mathcal{T}(\kappa,t)=-\kappa\Im[\hat{\overline{u}}^*(\hat{\overline{u}}\star\hat{\overline{u}})]$ the energy transfer among different resolved wave numbers, and $\mathcal{P}(\kappa,t)=-\kappa\Im[\hat{\overline{u}}\star\hat{\tau}]$ a source term due to the interaction between resolved and unresolved eddies. The resolved energy balance equation (8) shows the same form of the total energy equation (7), with exception of the appearance of the term $\mathcal{P}$, which involves the SGS model. When the sharp cutoff filter is adopted, $\mathcal{P}$ represents exactly the energy transfer between large and small scales while, for smooth filters, it must also account for large scale interactions. Then, in the ideal condition that velocity field has no energy beyond κ_c, the corresponding sharp cutoff filter does not alter the energy transfer, since $\mathcal{P}=0$ from $\hat{\tau}=0$. The same is no longer true for a smooth filter (with $\overline{\kappa}=\kappa_c$), for which a drain of energy due to filtering of large scales exists.

III. NUMERICAL EXPERIMENTS

A. DNS results

In order to make some numerical experiments, different realizations of a one-dimensional homogeneous velocity field were obtained integrating in time Eq. (1), starting from a given initial condition

$$u(x,0)=u_0(x), \quad -L/2\leqslant x<L/2, \tag{9}$$

with periodic boundary conditions

$$u(-L/2,t)=u(L/2,t), \quad t\geqslant 0. \tag{10}$$

The initial velocity field was assumed to have Gaussian statistics and generated by a white noise process, as proposed in Ref. 29. The initial energy spectrum was chosen to be $E(\kappa,0)=E_0(\kappa)=A\sigma^5\kappa^4\exp(-\kappa^2\sigma^2/2)$. In order to have $\int E_0(\kappa)d\kappa=1/2$, the constant A was set to $1/(3\sqrt{2\pi})$, while $\sigma=L/(40\pi)$ was chosen, so that the spectrum reached its maximum value at $40(2\pi/L)$.

The analytical solution of the Burgers equation (1) with the initial and boundary conditions (9) and (10) is known and given in Ref. 27. However, due to computer roundoff error it is practically impossible to accurately evaluate analytical solution for small values of ν. For that reason the numerical integration of Eq. (1) was carried out with a semidiscretized approach: a fourth order Runge–Kutta scheme was adopted for time integration while spatial derivatives were discretized by fourth-order central finite difference formulas. In order to have an energy conserving numerical scheme, the nonlinear term was discretized in the skew-symmetric form $(u\partial u/\partial x+\partial u^2/\partial x)/3$. DNS calculations were performed for a viscosity coefficient $\nu=5\times10^{-5}$. The mesh interval was set at $h=L/32\,768$ while the time step was set at $\Delta t=2\times10^{-6}$; 32 sample fields were simulated in time until the energy content of the flow was reduced to a few percent of the initial value. Note that in this paper we consider the case of freely decaying turbulent flow, since the governing equation (1) does not have a force term.

The initial energy density spectrum, together with the spectra at two following instants, $t=0.006$ and $t=0.03$, are reported in Fig. 1. Note that only the first 256 wave numbers were initially excited. As simulation goes on, higher wave numbers are involved and an inertial range, whose slope agrees well with the theoretical value -2,[30] is established. Finally, viscous dissipation takes place at the highest wave numbers. As illustrated in Fig. 2, the energy content of the flow $\mathbf{E}(t)=\int E(\kappa,t)d\kappa$ initially decreases slightly, corre-

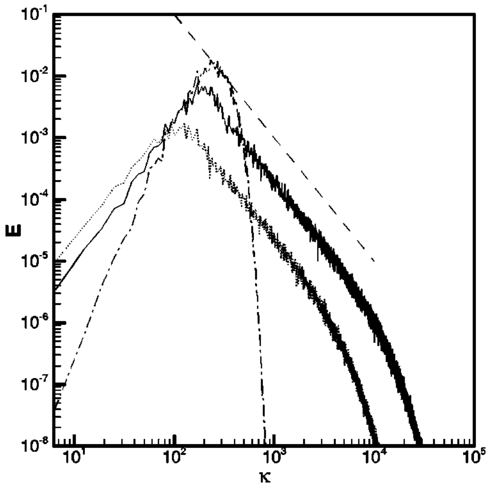

FIG. 1. Temporal evolution of energy density spectrum for DNS: $t=0$ $(-\cdot-)$, $t=0.006$ (—), $t=0.03$ $(\cdots)$; the ideal slope -2 is also shown for comparison.

sponding to the development of shock-like structures, then strongly, when the viscous dissipation occurs. The temporal evolution of total viscous dissipation $\mathbf{D}(t)=2\nu\int\kappa^2 E(\kappa,t)d\kappa$ is also reported in Fig. 2. As known, these two quantities are related by the relation $d\mathbf{E}/dt=-\mathbf{D}$, as readily obtained integrating Eq. (7) over all wave numbers.

The DNS results presented in this section will be used as a reference solution, and LES results presented in Sec. III B will be compared with the filtered DNS results. Furthermore, DNS data will be assumed as the exact solution of the Burgers equation (1) and a *perfect* SGS model will be constructed from DNS solution, say u_d, by using definition (4):

$$\tau_d(x,t)=\overline{u_d^2}-\overline{u}_d^2. \tag{11}$$

The discrete values in space and time of this function are stored in order to be used in *perfect* LES runs, as discussed in the following section.

B. LES results

When comparing LES results for different filters, it is important to make sure that these filters correspond to the same filter width. For that reason it is important to use consistent filter width definition. Typically, the definition of the filter width is based on the second moment of the filter kernel. However, there is a class of commutative filters (e.g., Ref. 5) that are close to sharp cutoff filter and have a number of zero moments. It was shown by Lund[31] that in the case of vanishing second moment the filter width can be accurately predicted from the associated transfer function. He suggested three different alternative methods for defining the filter width that give very similar results. In this paper we adopt the second definition: the filter width is taken to be proportional to the inverse wave number $\overline{\kappa}$, where the filter transfer function falls to 1/2.[31] This rule gives $\Delta=\pi/\overline{\kappa}$, as already considered in Sec. II. This definition is consistent and can be applied to smooth, close to sharp cutoff, and sharp cutoff filters.

LES calculations were performed starting from the filtered initial velocity field $\overline{u}_0$, for both sharp cutoff and smooth filters. In this study we use a top-hat filter as an example of smooth filters, since it is often employed in LES of turbulent flows. In order to avoid a strong influence of numerical errors on the solution, the mesh interval for LES simulation was chosen to be sufficiently small, i.e., $h'=64h$, while the filter width was chosen such that filter width to grid ratio for both sharp cutoff and smooth filters was $\mathrm{FGR}=\Delta/h'=3.3$. This way, we clearly kept the numerical and the filtering issues apart. In fact, since we used a finite difference numerical scheme, the highest wave number components of the velocity field are poorly simulated[32] and the truncation errors could be otherwise relevant. Note also that the filter width was such that $\kappa_c=\overline{\kappa}=77(2\pi/L)$ and the initial spectrum practically showed no energy beyond this wave number.

LES results were obtained from the solution of the filtered equation (3). Running LES supplied with the *perfect* SGS stress τ_d (11), we recover exactly the same energy spectra of filtered DNS solution, regardless of the filter used. Both spectra are shown, at $t=0.006$, in Figs. 3 and 4 for sharp cutoff and top-hat filter, respectively. The spectra of filtered DNS and *perfect* LES fields are practically the same as it results from analyzing the absolute difference, also reported in the Figs. 3 and 4. This is not surprising, since we

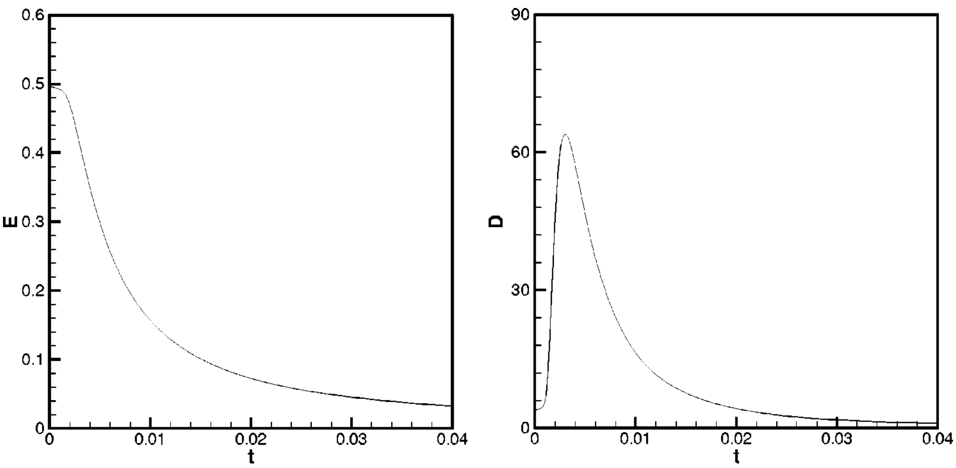

FIG. 2. Temporal evolution of total energy E and viscous dissipation D for DNS.

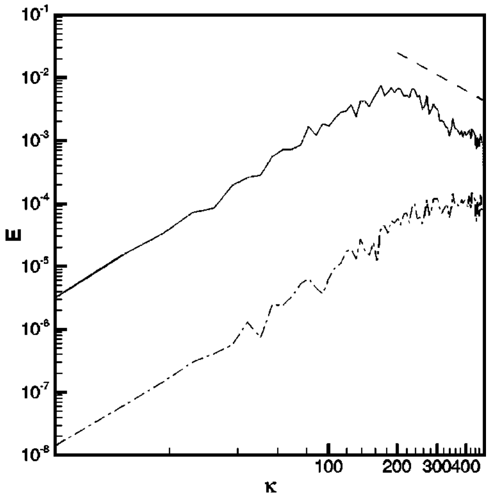

FIG. 3. Sharp cutoff filter: comparison between energy spectra at $t=0.006$ for filtered DNS (—) and *perfect* LES (···); their absolute difference (−·−) and the ideal slope -2 (−−−) are also shown.

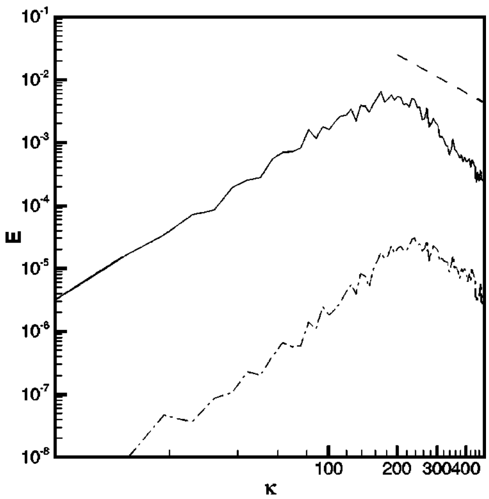

FIG. 4. Top-hat filter: comparison between energy spectra at $t=0.006$ for filtered DNS (—) and *perfect* LES (···); their absolute difference (−·−) and the ideal slope -2 (−−−) are also shown.

provided a *perfect* SGS model which gave us the exact dynamics and energy transfer, regardless of the filter used. Note also that, for the top-hat filter, even when the LES is conducted with this ideal SGS model, the resolved field loses some important features of the *real* field. For example, the slope of the inertial range is clearly misrepresented.

Figure 5 illustrates the temporal evolution of total energy and dissipation (viscous plus SGS dissipation) for *perfect* LES. The energy content of the resolved field changes in time according to $d\mathbf{E}/dt=-\mathbf{D}+\mathbf{P}$, where, without introducing other symbols, $\mathbf{E}$ stands for the total energy associated with the resolved scales, $\mathbf{D}$ the corresponding viscous dissipation, and $\mathbf{P}$ for the SGS dissipation: $\mathbf{P}=\int_{|\kappa|\leq\kappa_c}\mathcal{P}(\kappa,t)\,d\kappa =-\langle\overline{u(\partial\tau/\partial x)}\rangle$, as it results by integrating Eq. (8) over all resolved wave numbers. Note that $\langle\cdot\rangle$ stands for an ensemble average.

For the sharp cutoff filter, the solution keeps a high fraction of the energy content of the flow, while, for the top-hat filter, a large part of it is lost. Due to the perfect modeling and the good numerics exploited this loss of energy exactly accounts for the effect of smooth filtering on LES solution. Note that even if the initial spectrum is basically in the range of resolved scales, because of the unavoidable spreading of energy over higher wave numbers, smooth filtering causes a misrepresentation of energy cascade toward small scales. Moreover, a very large part of the dissipation is provided by the SGS model, as clearly illustrated in Fig. 6. This confirms how the success of the LES approach strongly depends on the accurate representation of the unknown SGS stress.

As a matter of fact, in performing LES one can only approximate in some way the contribution of this term. Thus, in order to mimic a real SGS model, in which it is hard to model large scales, we modified the *perfect* SGS stress (11) taking the effect of large scales out, but leaving the small ones intact. This was achieved by treating it with a high-pass discrete filter, whose Fourier transform was $1-\hat{G}(\kappa)$, being

$$\hat{G}(\kappa)=\sum_{n=-N}^{N} w_n e^{-i\tilde{\Delta}\kappa n}. \tag{12}$$

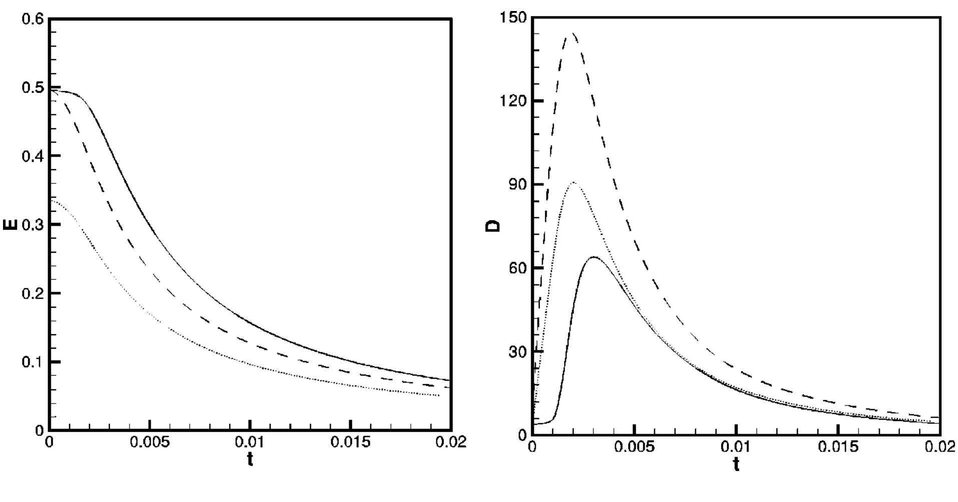

FIG. 5. Temporal evolution of total energy E and dissipation dE/dt for *perfect* LES, for both sharp cutoff (−−−) and top-hat (···) filters, together with those for DNS (—).

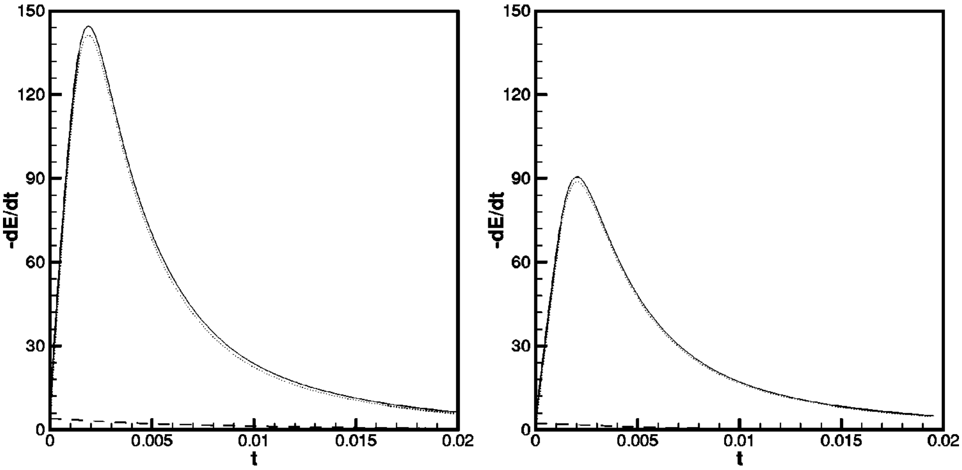

FIG. 6. Temporal evolution of viscous (– – –) and SGS dissipation (···) for *perfect* LES for both sharp cutoff (left) and top-hat (right) filters together with the total value (—).

Note that the filter could be chosen symmetric, owing to the fact the considered flow is homogeneous. A minimally constrained filter with five vanishing moments (with $N=3$) was adopted to alter the SGS model. The weight factors w_n were those given in Ref. 5, namely corresponding to case 10 in Table I of Ref. 5. The high-pass filter width $\tilde{\Delta}$ was chosen to be 1.2, 1.8, and 2.4 times the LES filter width Δ. For increasing values of $\tilde{\Delta}$ more scales were left intact and the *perfect* LES was approached.

Results for LES with modified SGS model, in terms of total energy and dissipation evolution, are presented in Figs. 7 and 8. Altering the *perfect* SGS model causes a wrong evolution of total energy: the dissipation provided by the model was not enough and kinetic energy decays less in time with respect to the perfect case. To demonstrate the effect of the filter shape on the energy spectrum, we considered in Figs. 9 and 10 the energy spectra of the altered LES fields, for both sharp cutoff and top-hat filtering. The time instant was the same as for the previous analogous figures. While the energy density spectrum is little modified by altering the SGS model for sharp cutoff LES, the same is not true for the top-hat LES. In the latter case, marked differences appear also at low wave numbers and the differences between the two filtering approaches are enhanced by increasing the high-pass filter width $\tilde{\Delta}$. Note that for sharp cutoff filtering, according to Eq. (6), the SGS stress has a very little contribution from large scales, therefore the modified SGS model remains a good model even in its altered form.

Finally, the presented diagnostics clearly demonstrate that if smooth filters are used for LES, then one needs to account for the large scale effects as well. Thus, there are two choices: either to use filters close to sharp cutoff filters, or to develop special models that take into account large scale structures, even though the latter approach would be very similar in spirit to unsteady RANS.

IV. CONCLUSIONS

In this study we carried out the numerical simulations, both DNS and LES, of the solution of one-dimensional Burgers problem with periodic boundary conditions. Even if one can doubt this equation is a model for real three-dimensional turbulence, e.g., yielding a different energy spectrum, nevertheless it can be considered as a good test to address some issues in the numerical simulation of turbulence. As a matter of fact, the conclusions of the present study about the influence of the filter shape in LES do not depend on the simplified model considered. However, analogous numerical tests will be performed in the future for a three-dimensional homogeneous turbulent flow in order to confirm our conclusions.

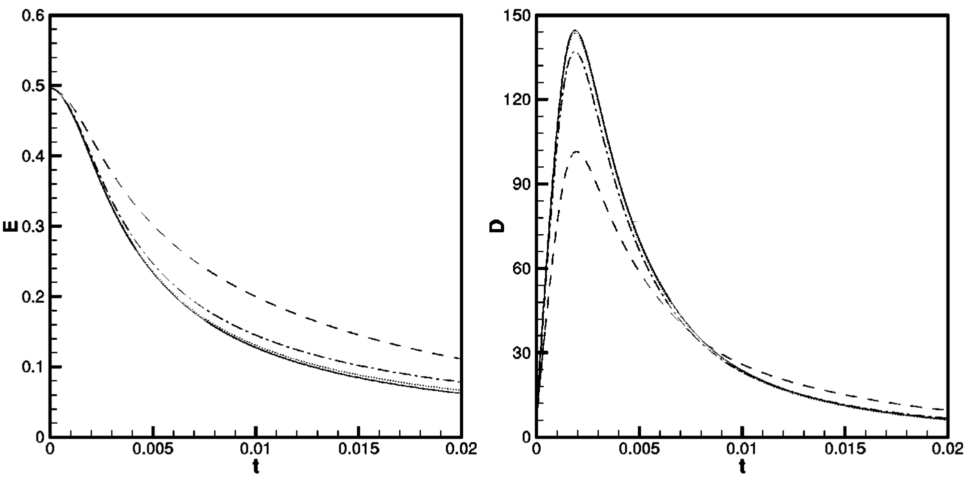

FIG. 7. Sharp cutoff filter: temporal evolution of total energy E and dissipation dE/dt for *perfect* LES (—) and altered LES with different ratios $\tilde{\Delta}/\Delta$: 1.2 (– – –), 1.8 (– · –) and 2.4 (···).

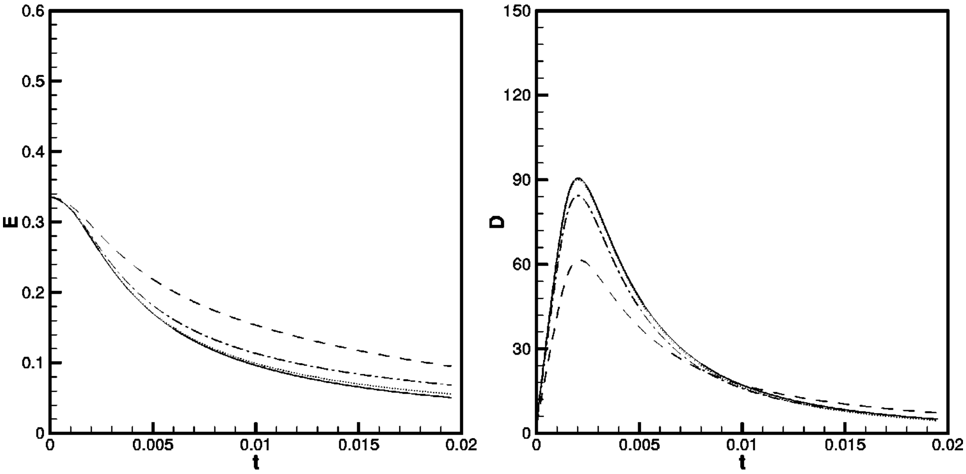

FIG. 8. Top-hat filter: temporal evolution of total energy E and dissipation dE/dt for *perfect* LES (—) and altered LES with different ratios $\tilde{\Delta}/\Delta$: 1.2 (– – –), 1.8 (– · –) and 2.4 (···).

It is worth noting how the analysis was conducted not by means of *a priori* tests, as often made in similar studies, but performing actual large eddy simulations with SGS models obtained by filtering DNS results. This way, one can follow the dynamical interactions between the flow simulation and the adopted modeling procedure.

A high-order nondissipative numerical method and a sufficiently fine grid were employed in order to minimize the influence of truncation and aliasing errors. First, we used a *perfect* SGS model constructed by definition upon the DNS solution, considered as the exact solution. This way, the pure effect of filtering on actual LES solution could be illustrated. Then, in order to mimic a real simulation, the ideal SGS model was altered by filtering out the contribution of large scales on it.

Both theoretical and numerical results presented in this paper have clearly demonstrated the importance of considering SGS modeling and filtering as an inseparable issue. In particular, it was shown that if LES is based on a smooth filter, then the SGS model should also model the effect of the filter on large scales, i.e., forces (stresses) produced by interaction of large scales which are filtered out. The same is for energy cascade: SGS model should remove (or add) energy at the resolved scales due to the simple fact that filtering procedures remove them. This contradicts the basic motivation behind LES: to resolve large scales and model unresolved ones. One should not model the interaction of resolved scales, otherwise it will be hard to see the difference between unsteady RANS and LES. However, unless one considers homogeneous turbulence, it is difficult, if not impossible, to adopt an implicit or explicit sharp cutoff filter. Then, the next best choice is to minimize the effect of filter on large scale dynamics and energy transfer. This can be achieved by making the filter as close to sharp cutoff as possible.

It is worth stressing how, alternatively, one could also abandon the physical point of view and think to simulate filtered velocity dynamics, without introducing a formal separation between large and small scales. In this case, τ still defines the effect of the unresolved part of the field on the resolved one but, for smooth filters, it no longer has the meaning of a subgrid scale stress, even if the latter term is usually still adopted (and the approach is still called LES). From this point of view, there would be no substantial con-

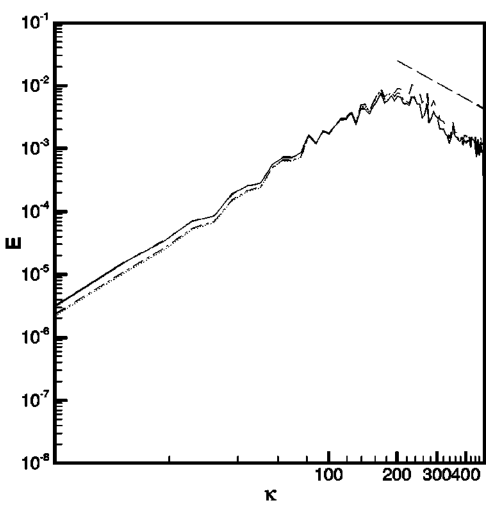

FIG. 9. Sharp cutoff filter: energy spectrum at $t=0.006$ for *perfect* LES (—) and altered LES with different ratios $\tilde{\Delta}/\Delta$: 1.2 (– – –), 1.8 (– · –), and 2.4 (···).

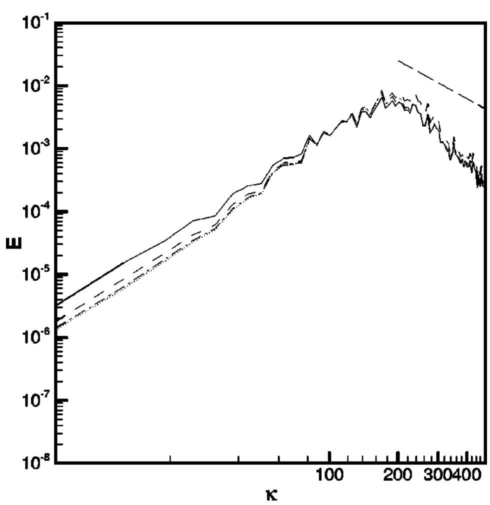

FIG. 10. Top-hat filter: energy spectrum at $t=0.006$ for *perfect* LES (—) and altered LES with different ratios $\tilde{\Delta}/\Delta$: 1.2 (– – –), 1.8 (– · –), and 2.4 (···).

ceptual difference between any kind of filter and the matter would consist only in defining a good model for the unknown stress term.

ACKNOWLEDGMENTS

The authors thank Thomas Lund for helpful discussion. O.V. was supported by the University of Missouri Research Board Grant. This support is gratefully acknowledged.

[1] T. S. Lund and H.-J. Kaltenbach, ‘‘Experiments with explicit filtering for LES using a finite-difference method,’’ in *Annual Research Briefs*, Center for Turbulence Research, NASA Ames/Stanford University, 1995, p. 91.

[2] M. Germano, U. Piomelli, P. Moin, and W. Cabot, ‘‘A dynamic subgrid-scale eddy-viscosity model,’’ Phys. Fluids A **3**, 1760 (1991).

[3] S. Ghosal, T. S. Lund, P. Moin, and K. Akselvoll, ‘‘A dynamic localization model for large-eddy simulation of turbulent flows,’’ J. Fluid Mech. **286**, 229 (1995).

[4] S. Ghosal, ‘‘An analysis of numerical errors in large eddy simulations of turbulence,’’ J. Comput. Phys. **125**, 187 (1996).

[5] O. V. Vasilyev, T. S. Lund, and P. Moin, ‘‘A general class of commutative filters for LES in complex geometries,’’ J. Comput. Phys. **146**, 105 (1998).

[6] J. Bardina, J. H. Ferziger, and W. C. Reynolds, ‘‘Improved turbulence models based on large eddy simulation of homogeneous incompressible turbulence,’’ Report No. TF-19, Thermosciences Division, Department of Mechanical Engineering, Stanford University, 1983.

[7] W. K. Yeo and K. W. Bedford, ‘‘Closure-free turbulence modeling based upon a conjunctive higher order averaging procedure,’’ *Computational Methods in Flow Analysis*, edited by H. Niki and M. Kawahara (Okayama University Press, Okayama, Japan, 1988), pp. 844–851.

[8] K. W. Bedford and W. K. Yeo, ‘‘Conjunctive filtering procedures in surface water flow and transport,’’ in *Large Eddy Simulation of Complex Engineering and Geophysical Flows*, edited by B. Galperin and S. A. Orszag (Cambridge University Press, Cambridge, 1993), pp. 513–537.

[9] A. Leonard, ‘‘Energy cascade in large-eddy simulations of turbulent fluid flows,’’ Adv. Geophys. **18**, 237 (1974).

[10] A. Leonard ‘‘Large-eddy simulation of chaotic convection and beyond,’’ *35th Aerospaces Sciences Meeting and Exhibit*, 6–10 January 1997, Reno, NV, AIAA Paper No. 97-0204.

[11] R. A. Clark, J. H. Ferziger, and W. C. Reynolds, ‘‘Evaluation of subgrid-scale turbulence models using an accurately simulated turbulent flow,’’ J. Fluid Mech. **91**, 1 (1979).

[12] K. Horiuti, ‘‘The role of the Bardina model in large eddy simulation of turbulent channel flow,’’ Phys. Fluids A **1**, 426 (1989).

[13] S. Liu, C. Meneveau, and J. Katz, ‘‘On the properties of similarity subgrid-scale models as deduced from measurements in a turbulent jet,’’ J. Fluid Mech. **275**, 83 (1994).

[14] M. Salvetti and S. Banerjee, ‘‘*A priori* tests of a new dynamic subgrid-scale model for finite-difference large-eddy simulations,’’ Phys. Fluids **7**, 2831 (1995).

[15] G. S. Winckelmans, T. S. Lund, D. Carati, and A. A. Wray, ‘‘*A priori* testing of subgrid-scale models in the velocity-pressure and the vorticity-velocity formulations,’’ Proceedings of the Summer Program, Center for Turbulence Research, 1996 (Stanford University and NASA Ames), pp. 309–328.

[16] G. S. Winckelmans, A. A. Wray, and O. V. Vasilyev, ‘‘Testing of a new mixed model for LES: the Leonard model supplemented by a dynamic Smagorinsky term,’’ Proceedings of the Summer Program, Center for Turbulence Research, Stanford University and NASA Ames, pp. 367–388.

[17] G. S. Winckelmans, A. A. Wray, O. V. Vasilyev, and H. Jeanmart, ‘‘Explicit-filtering large-eddy simulation using the tensor-diffusivity model supplemented by a dynamic Smagorinsky term,’’ Phys. Fluids **13**, 1385 (2001).

[18] Y. Zang, R. L. Street, and J. R. Koseff, ‘‘A dynamic mixed subgrid-scale model and its application to turbulent recirculating flows,’’ Phys. Fluids A **5**, 3186 (1993).

[19] B. Vreman, B. Geurts, and H. Kuerten, ‘‘On the formulation of the dynamic mixed subgrid-scale model,’’ Phys. Fluids **6**, 4057 (1994).

[20] B. Vreman, B. Geurts, and H. Kuerten, ‘‘Large-eddy simulation of the temporal mixing layer using the mixed Clark model,’’ Theor. Comput. Fluid Dyn. **8**, 309 (1996).

[21] B. Vreman, B. Geurts, and H. Kuerten, ‘‘Large-eddy simulation of the turbulent mixing layer,’’ J. Fluid Mech. **339**, 357 (1997).

[22] K. Horiuti, ‘‘A new dynamic two-parameter mixed model for large-eddy simulation,’’ Phys. Fluids **9**, 3443 (1997).

[23] Y. Morinihsi and O. V. Vasilyev, ‘‘A recommended modification to the dynamic two-parameter mixed subgrid scale model for large eddy simulation of turbulent flow,’’ Phys. Fluids **13**, 3400 (2001).

[24] J. S. Smagorinsky, ‘‘General circulation experiments with the primitive equations,’’ Mon. Weather Rev. **91**, 99 (1963).

[25] G. Dantinne, H. Jeanmart, G. S. Winckelmans, V. Legat, and C. Carati, ‘‘Hyperviscosity and vorticity-based models for subgrid scale modeling,’’ Appl. Sci. Res. **59**, 409 (1998).

[26] U. Piomelli, P. Moin, and J. H. Ferziger, ‘‘Model consistency in large eddy simulation of turbulent channel flows,’’ Phys. Fluids **31**, 1884 (1988).

[27] J. M. Burgers, *The Nonlinear Diffusion Equation* (Reidel, Dordrecht, 1974).

[28] M. D. Love, ‘‘Subgrid modeling studies with Burgers equation,’’ J. Fluid Mech. **100**, 87 (1980).

[29] D. T. Jeng, ‘‘Forced model equation for turbulence,’’ Phys. Fluids **12**, 2006 (1969).

[30] S. N. Gurbatov, S. I. Simdyankin, E. Aurell, U. Frisch, and G. Toth, ‘‘On the decay of Burgers turbulence,’’ J. Fluid Mech. **344**, 339 (1997).

[31] T. S. Lund, ‘‘On the use of discrete filters for large eddy simulation,’’ Center for Turbulence Research Annual Research Briefs, 1997, pp. 83–95.

[32] A. G. Kravchenko and P. Moin, ‘‘On the effect of numerical errors in large eddy simulations of turbulent flows,’’ J. Comput. Phys. **131**, 310 (1997).